ICES annual conference, Aberdeen 20-24. Sept. 2005
ICES CM 2005/Sesson O:26

Connecting Physical-Biological Interactions to Recruitment Variability, Ecosystem Dynamics, and the Management of Exploited Stocks

Swell as a turbulence source in shallow water

Jan Erik Stiansen [1], Svein Sundby [1], Alastair D. Jenkins [2] and Jan Even Øie Nilsen [3]

Contact author:
Jan Erik Stiansen, Institute of Marine Research, PO box 1870, 5817 Bergen, Norway [Tel: +47 55 23 85 00, e-mail: jan.erik.stiansen@imr.no]

Keywords: swell, turbulence, energy dissipation rate, zooplankton, fish larvae

Abstract

Two field investigations in an exposed shallow area outside Lofoten, western Norway, were conducted in 1995 and 1996. Direct measurements of turbulence were conducted from an underwater tower with acoustic current meters 6 m above the bottom. The tidal energy in this area is low and the wind conditions during the experiment were mostly weak. Nevertheless, the turbulent kinetic energy dissipation rate at 20-25 m depth was in the range 10^{-7}-10^{-5} W/kg. The only other possible energy source was long swell of wavelength 100-200 m that rolled in from the open sea. Analysis shows that the wave related water motion intermittently becomes unstable, inducing strong turbulent patches in parts of the wave orbit. The mechanism behind this process is not clear, but possible explanations may be local energy concentration or interaction of waves with different frequency. In many areas and situations this energy source is equal in force to tidal and wind generated turbulence. Simultaneous measurement of vertical profiles of zooplankton and fish larvae from a nearby location enables us to discuss swell-induced turbulence in an ecological context.

Addresses of authors:
[1] Institute of Marine Research (IMR), PO box 1870 Nordnes, 5817 Bergen, Norway.
[2] Bjerknes Centre for Climate Research, Geophysical Institute, Allegaten 70, 5007 Bergen, Norway.
[3] Nansen Environmental and Remote Sensing Center (NERSC), Thormøhlensgt. 47, 5006 Bergen, Norway.

Introduction

The coastal waters around the Lofoten archipelago are the major first-feeding areas for larval Arcto-Norwegian cod. Physically, the larval habitat can be divided in four categories. The major part of the habitat consists of relatively deep open coastal waters with water depth more than 50 m close to shore and abruptly increasing to more than 200 m depth. Here, turbulence is dominated by the variable wind forcing. In the more sheltered inlets and fjords with depths of 50-150 m, the wind-induced turbulence also dominates, but the energy dissipation rate is generally smaller due to more shelter against the wind. The third category is the shallow tidal sound of water depth less than 50 m. Here, turbulence is dominated by strong tidal forces, particularly in the Moskenesstraumen where tidal current speed may exceed 7 knots over 40 m bottom depth. The fourth category is a shallow bank region of bottom depth 20-30 m bounded by the tidally energetic Gimsøystraumen in south and open coastal waters to the north and west. This is the study site of the present investigation. Here, we observed at particular times the turbulence to be dominated by swell-induced turbulence. The peculiar feature in this region is the presence of intermittently occurring turbulence, i.e. strong release of turbulent energy at short periods and with very low turbulent intensities in between.

The turbulence generated by swell (long surface gravity waves generated by wind forcing at a remote location) seems to take place within the water column. The precise mechanisms are not yet, clear, but the turbulence is characterised by small-scale patchiness, short timescales and intermittency. In this paper we will try to elucidate the phenomenon by presenting some preliminary results.

Material and methods

Surveys were conducted the first week of May at the same location, outside Lofoten, western Norway, in two successive years (1995 and 1996). This is at the peak time of hatching of northeast arctic cod larvae. The area investigated is a shallow plateau in the drift path of the larvae, just north of the spawning site. The intention of the investigation was to study the effect of turbulence on larval feeding (e.g. predator-prey encounters).

The investigation may be divided into two parts each year. Firstly, a ship survey (R/S *G. O. Sars* in 1995 and R/S *Johan Hjort* in 1996), tracking the egg and larvae concentrations. Secondly, a site investigation where the ship lay by anchor and an underwater tower with turbulence current meters was deployed nearby. In this paper we will focus on the second part of the investigation, with the underwater tower and the ship at anchor, and only for the investigation from 1995.

Four anchor stations were used (see Fig. 1): one at a very exposed area, two at medium/high exposed area, and one in a sheltered fjord. One of the stations was visited twice. All locations were in shallow water, between 20 and 30 m depth. The plateau was flat, with small stones and silt. The bottom in the sheltered fjord was also flat, but with more mud and sand.

The underwater tower (Fig. 2) was 6 m high, with 3 different high resolution acoustic current meters (an Ocean ADV from NORTEK, an MINILAB and an UCM from SimTronix) placed at the top, facing upwards in order to minimize the effects of the construction on the observations. In the middle of the tower a MiniCTD was placed. In an array from 1 m to 4 m above the bottom, within the tower, four SD6000 were placed. Accoustic instrumentation and

measurement prisniples are describes by Gytre *et al.* (1996). During the investigation the Ocean ADV malfunctioned, and also there were also intermittent problems with the MINILAB. Fortunately, the UCM functioned very well throughout the investigation.

The anchored ship took rapid vertical profiles of hydrography with a CTD, zooplankton with vertical hauled nets and fish larvae and zooplankton from specific depths with a large plankton pump ("Hufsa"). Meteorological data were sampled with the ship weather station (wind speed and direction). Around the plateau, three rigs with Aanderaa current meters were deployed.

The UCM was set at the highest measuring frequency of 2 Hz. The underwater data recorder could be deployed for about 16 hours at this rate before the memory capacity was filled up. The time series were split into 20 min series before spectral analysis was conducted. The energy dissipation rate was then calculated from the energy spectra according to the linear regression method by Stiansen and Sundby (2001), with the constant B set to 1 as was suggested by Stiansen and Sundby (2001).

The cod larvae were fixated on the ship, and later the gut content were analysed for prey species and size.

Results and discussion

The turbulence energy analysis (Fig. 4) shows large intensity difference between the different locations. In the sheltered fjord the there was little wave motion, and also little wind waves, tidal motion was also low (SD6000 data, not shown). This is also reflected in the low turbulence intensity (Fig. 4). At the exposed outer locations, swell wave trains rolled in from the open ocean. A 20-minute time series is shown as an example (Fig. 5). For most of the investigation period the wind was weak, and the wave field was dominated by swell.

Tidal model simulations by Bjørn Gjevik (Fig.1) show weak tidal currents on the plateau, except in an area just north of the island strait. During most of the investigation there was either no wind or weak winds. The source of the strong turbulence on the plateau could therefore not be due to either wind or tide. Forecasts from the Norwegian Meteorological Institute (Fig. 3) showed that large swell from the north-northeast were present at the location. This is also evident in the time series from the current meter (Fig. 5) and the energy spectra (Fig. 6). Energy spectra (Fig. 6) show a strong increase in turbulent energy (clear $f^{-5/3}$ inertial subrange) at lower frequencies than the wave range compared to lower frequencies. Waves with periods of about 8-12 sec are evident in the two horizontal components, but not in the vertical component, where the inertial subrange extends down to the swell frequency. Snapshots of the time series (Figs. 7 and 8) show intermittent strong instabilities in the wave oscillation velocity. This leads us to conclude that the swell in some way must be the turbulence source.

The mechanism behind this process is not clear, but possible explanations may be local energy concentration, interaction of waves with different frequency, or advection of turbulent motions from the turbulent bottom boundary layer generated by the swell-wave orbital

motions[1]. What seems clear is that it is a local instability. Contrary to wind-generated and tidally generated turbulence, which is generated at the boundaries and advected further into the open volume, this phenomenon occurs in the interior of the water column.

The exposed area is in general well mixed. However, weak stratification was at times present, and cannot for the moment be ruled out as a necessary factor for the swell-induced turbulence. Hydrographic sampling was conducted with a CTD instrument every 30 minutes at each anchor station. However, these data have not yet been analysed.

The number of prey organisms in the larval gut (Tables 1, Figs. 8 and 9) shows large differences among the anchor stations. The greatest number of organisms in the gut were found at the most sheltered location. At the more exposed locations there were also differences. These differences are not only dependent on the turbulence intensity, but also on the available prey (nauplii) concentration in the sea (Fig.9). At present this has not been addressed. It is therefore too early in the analysis to make any conclusions about the effect of turbulence on predator-prey relations. However, as the larvae grow, they may switch to larger prey containing more energy. The nauplii in the gut at the sheltered location at anchor station 4 were in general much smaller than those in the gut at the exposed locations. In terms of energy content in the larval gut (Tab. 1, Fig. 9) the difference between the anchor stations is much smaller.

The calculated energy dissipation rate must be seen as average values. The short-time patchiness of the turbulence combined with advection past the current meter makes it impossible to extract the dissipation rates of the actual turbulence burst, which must have a much higher intensity. In calculations of predator-pray relations it is usual to use mean energy dissipation rates. It remains an open question what effect such bursts have on the behaviour patterns of the larvae.

How common is this phenomenon? If we assume that the generating mechanism is entirely due to swell, this phenomenon may occur frequently at all exposed areas shallower than 50-100 m. On the other hand, if the generating mechanism also depends on wind-wave interaction and/or on a density gradient, the occurrence will be limited to much shallower waters and/or also limited in time to the necessary hydrographical conditions. Distinguishing between these mechanisms will require further fieldwork and theoretical investigations.

References

Stiansen,J.E. and S. Sundby, 2001. Improved methods for generating and estimating turbulence in tanks suitable for fish larvae experiments. *Scientia Marina*, 65 (2): 151-167.

Gytre,T., Nilsen, J.E.Ø., Stiansen,J.E. and Sundby,S (1996). Resolving Small Scale Turbulence with Acoustic Doppler and Acoustic Travel Time Difference Current Meters from an Underwater Tower. Proc. Oceans-96, *IEEE* p.442-50.

1 The oscillatory current motions shown in the sample time series have a period of about 16 seconds. Surface waves of this period have a wavelength of about 400 meters in deep water, and the orbital motions will extend downwards about 60 meters. Since the water depth of the reported field investigations was 20-25 m, the wave orbital motions will extend throughout the water column, and are highly likely to generate substantial turbulence in the bottom boundary layer. The extent to which the bottom turbulence is advected into the water column by a "bursting" process during the wave cycle will be the subject of a more detailed subsequent investigation.

Tables and Figures

Table 1. Statistics of larval gut content, nauplii sea concentration and average turbulence intensity.

Anchor station	Mean length cod	Mean number of nauplii in gut	Concentration of nauplii in seawater	Mean length of nauplii	Mean turbulence intensity	Energy per nauplius	Mean energy in cod gut
	mm		l^{-1}	µm	W/kg	J	J
I	46.85	1.89	11.22	299	1.12E-06	0.065	0.122
II	48.00	1.28	9.17	299	3.63E-06	0.065	0.083
III	47.06	1.56	15.48	275	3.39E-05	0.053	0.083
III-1	47.23	1.86	19.74	245	5.44E-05	0.041	0.076
III-2	47.00	1.45	13.59	306	1.7E-05	0.068	0.099
IV	42.21	3.43	7.90	214	4.25E-08	0.030	0.104
V	46.89	1.39	3.25	263	2.47E-06	0.048	0.067

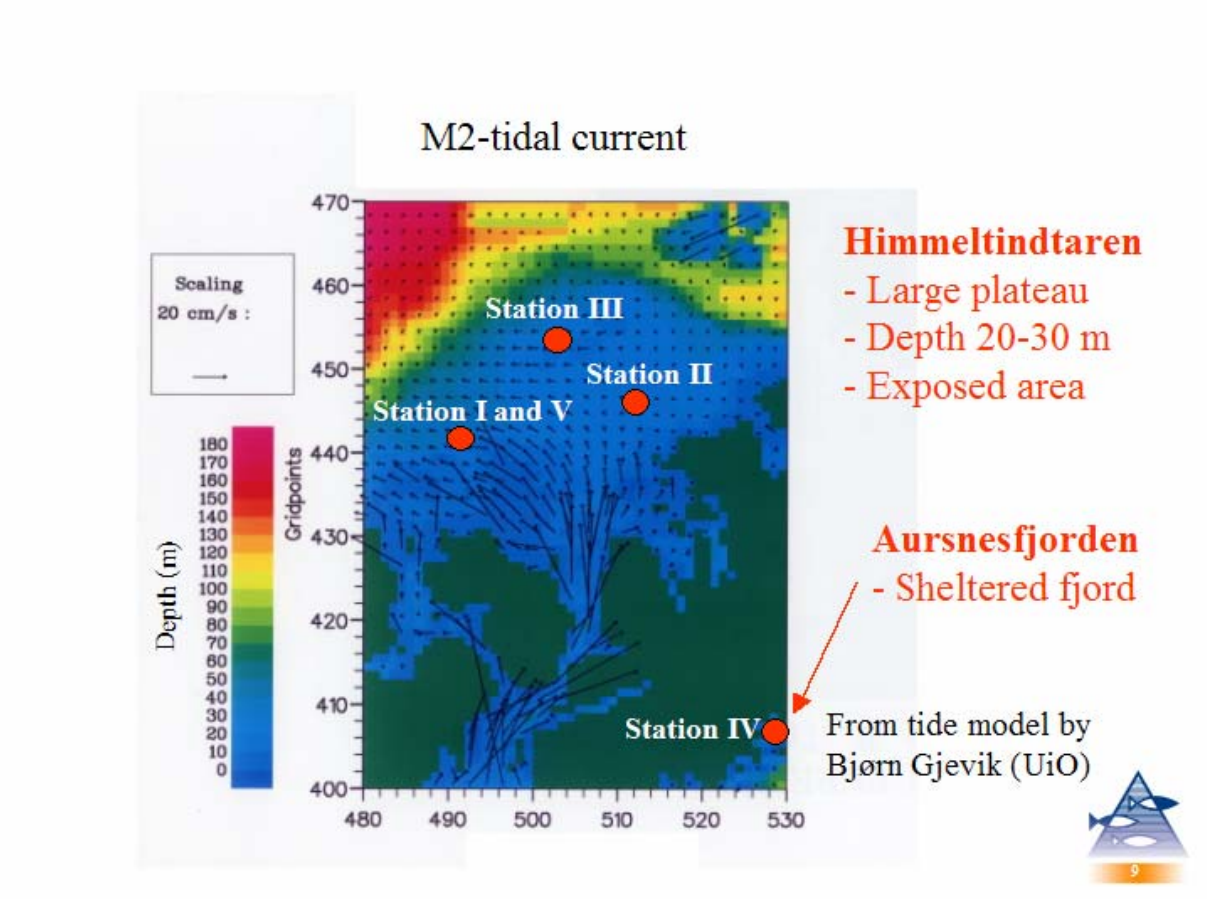

Figure 1. Overview of the investigation area. Colours indicate the depths at the location, arrows is the M_2 modelled tidal current (courtesy of Bjørn Gjevik, University of Oslo, Norway). Red dots are the different stations where the tower was used. Note that station IV is at the end of a south-facing fjord.

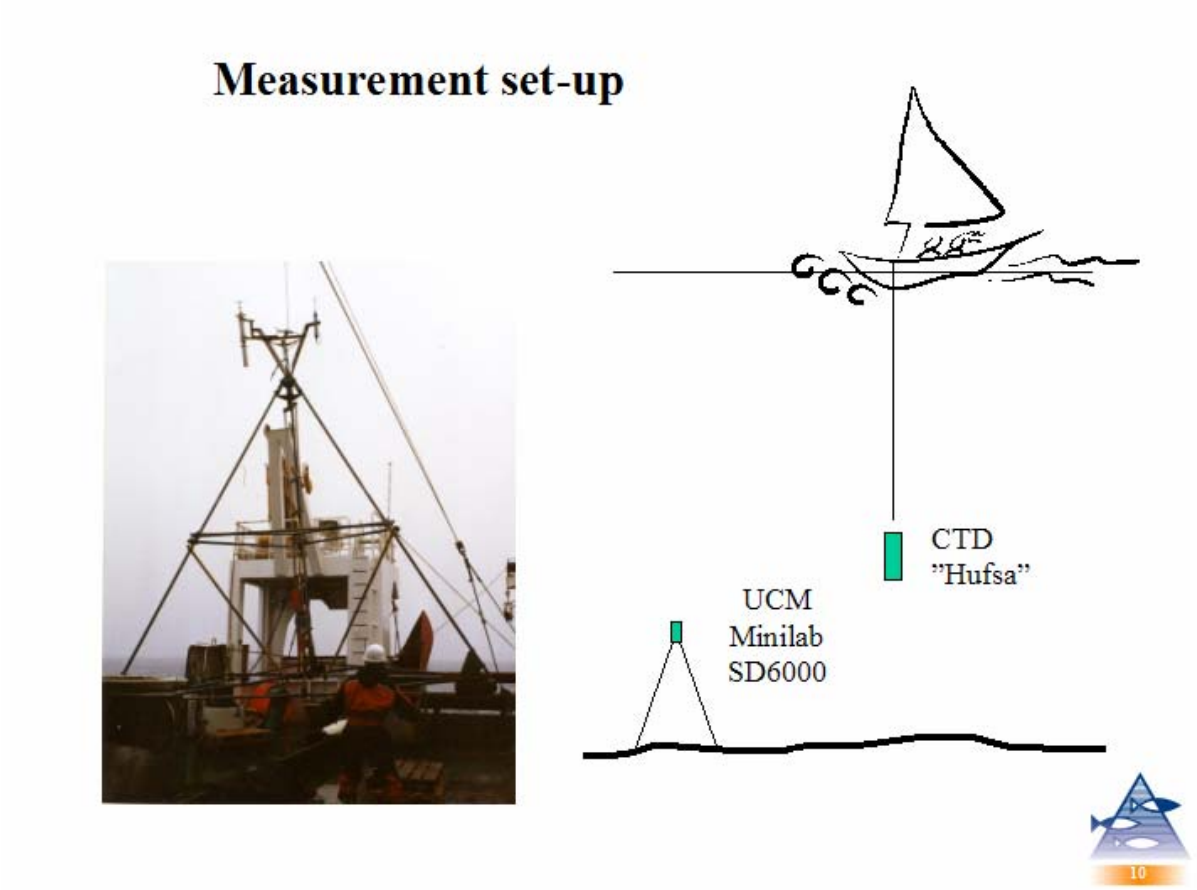

Figure 2. The left-hand picture shows the underwater tower before deployment (please note that the white structure in the background is a crane on the ship, and not part of the tower). The right-hand drawing is a sketch of the set-up.

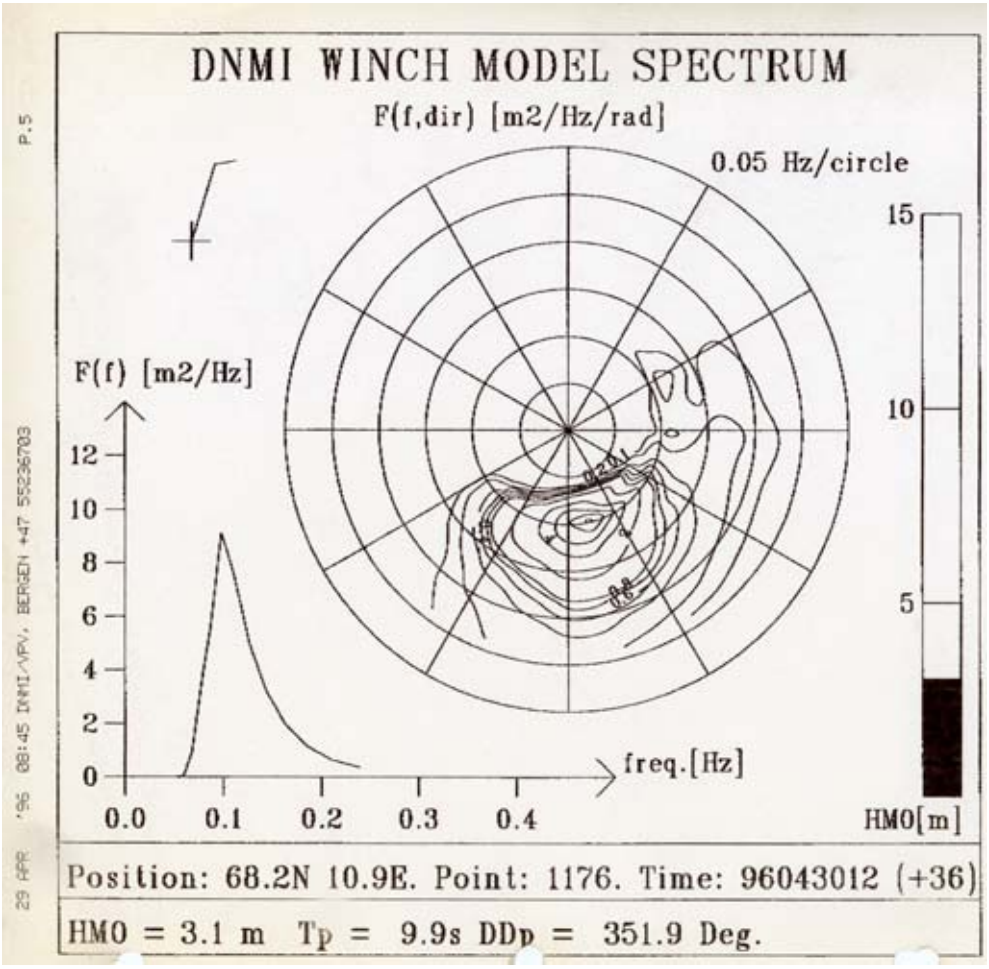

Figure 3. A wave forecast for the investigation area issued by the Norwegian Meteorological institute during the survey.

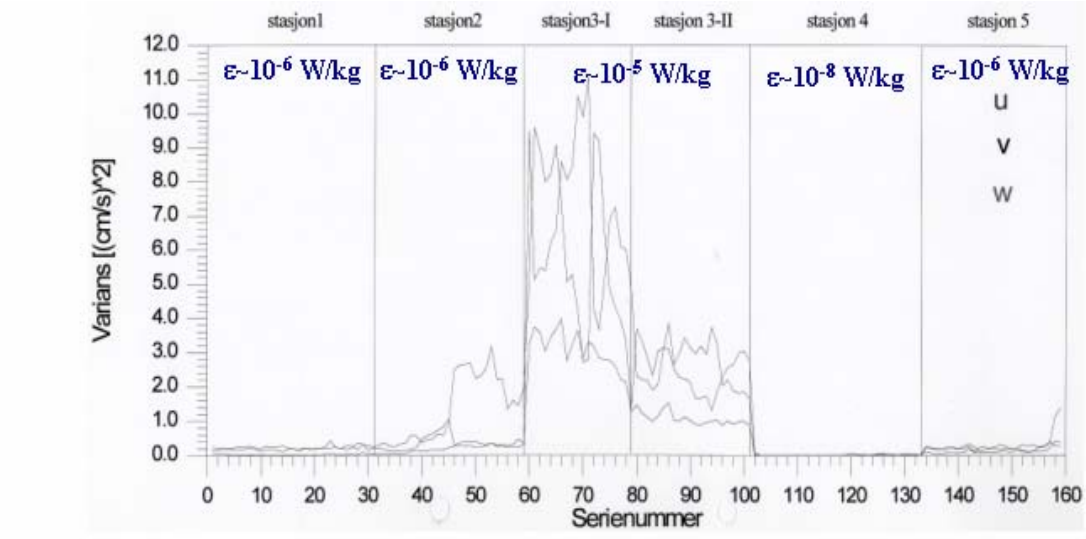

Figure 4. Variance from high-pass filtered (4.5 sec) time series (20 min) for the investigation period. The vertical lines separate the different anchor stations. Note that the X-axis is sample number, not time.

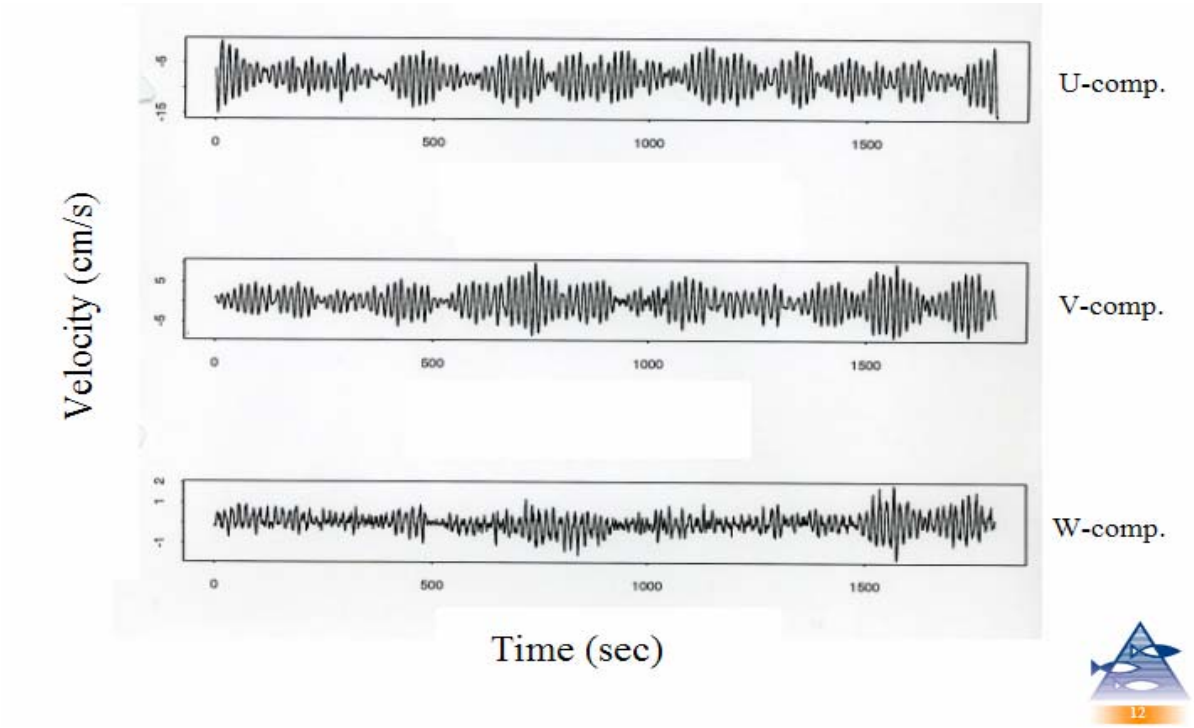

Figure 5. Example of a 20-minute time series for the three velocity components.

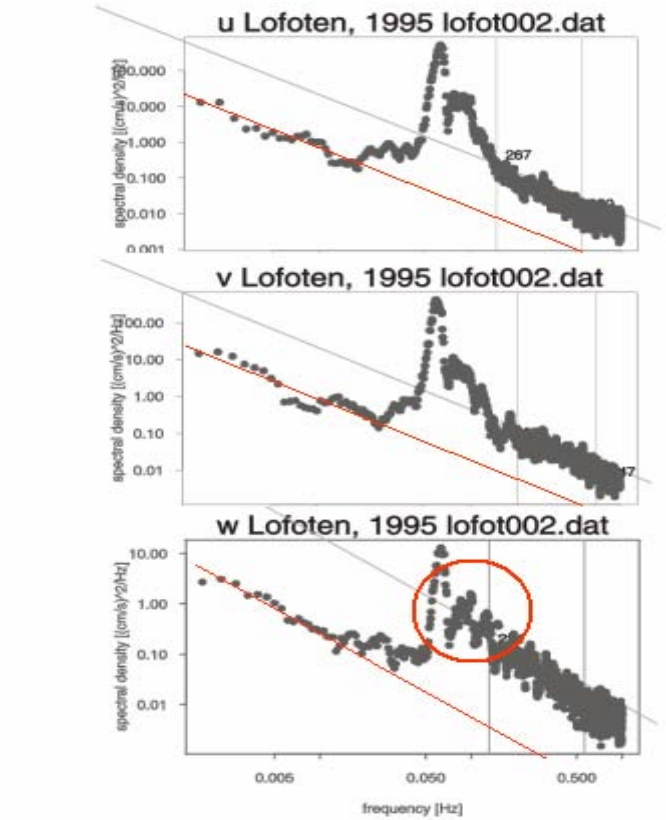

Figure 6. Example of energy spectra for the three velocity components. The red ring circles the range where the wind waves are damped out in the vertical component, due to the instrument depth of about 20 m. Note that the Y-axis scale of the figures are not equal.

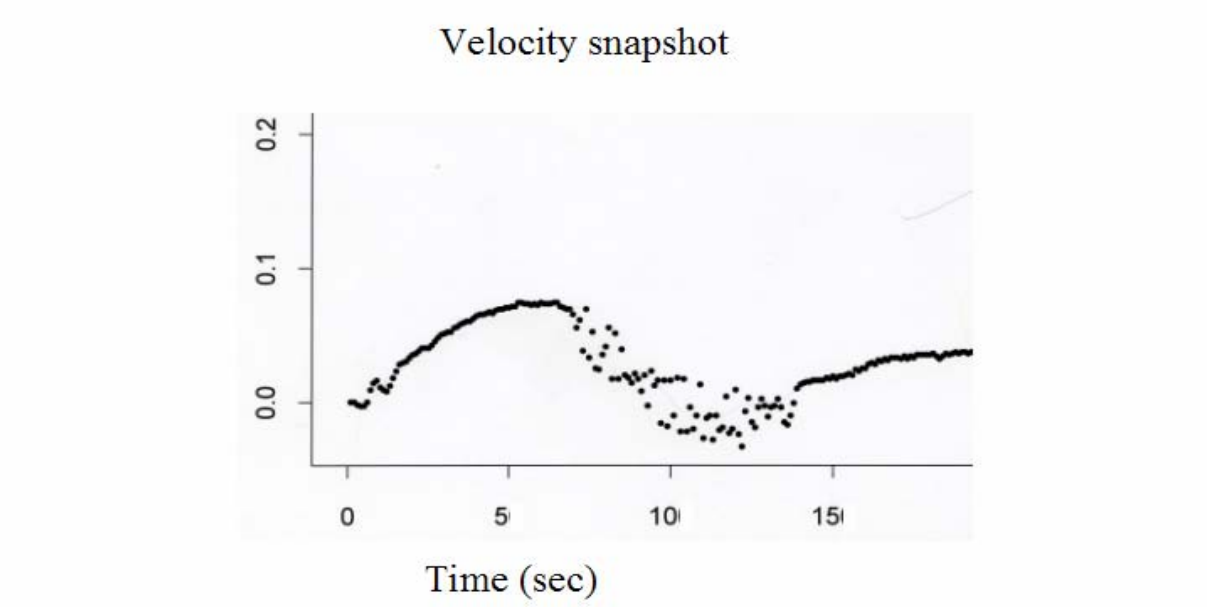

Figure 7. 20-second snapshot of a time series. This particular snapshot was our first view of this phenomenon, and was shown on our PC screen due to a typing error.

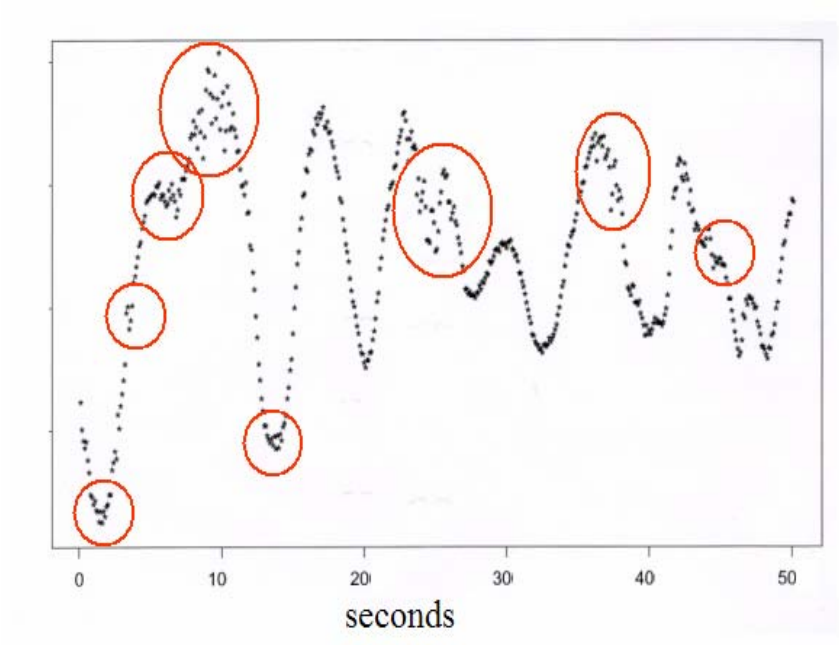

Figure 8. A 50-second snapshot of another time series. The red circles mark the occurrence of the turbulence phenomenon.

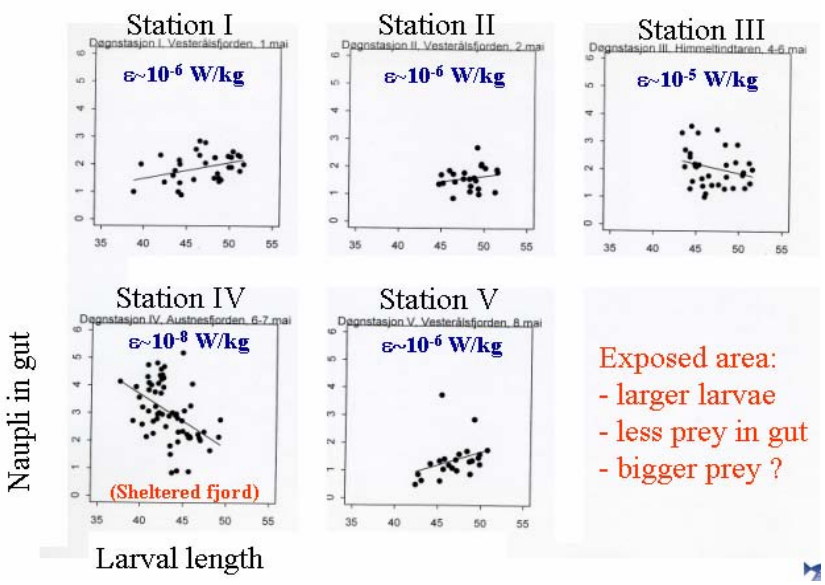

Figure 8. Number of nauplii in gut vs. length of the cod larvae for the different anchor stations.

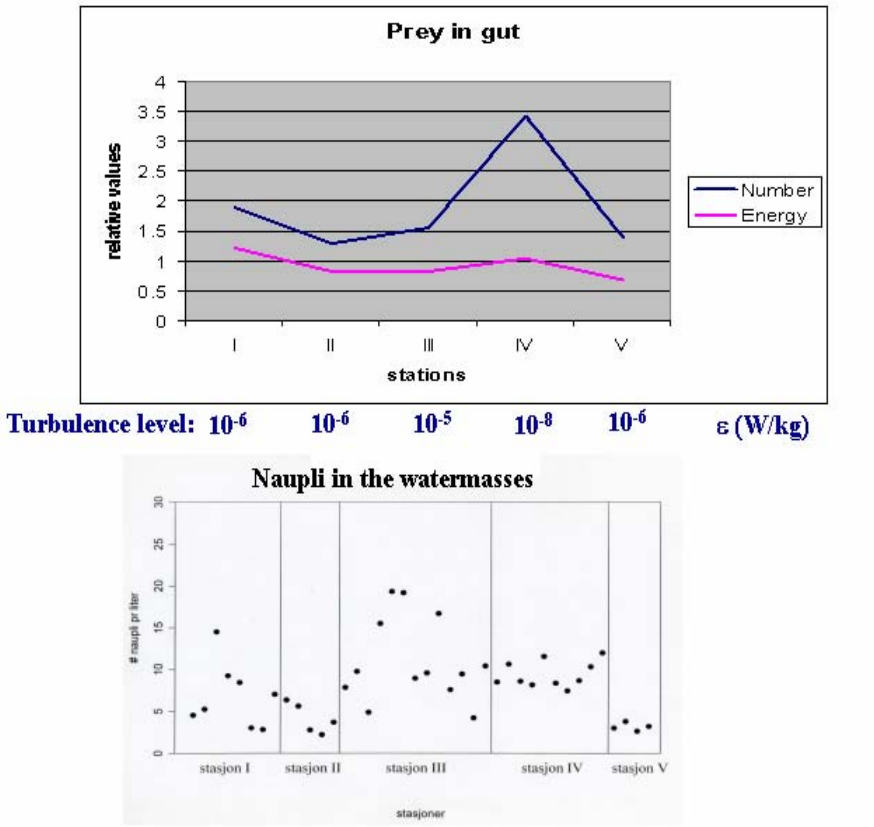

Figure 9. Upper panel shows the number of nauplii in the gut (blue line) and the associated energy content (red line) in the cod gut at the different anchor stations. The lower panel shows the number (concentration) of nauplii in the water column for each sample at the different anchor stations. The related energy dissipation rate at each anchor station is indicated between the upper and lower panels.